Available online at www.sciencedirect.com

ScienceDirect

IFAC PapersOnline CONFERENCE PAPER ARCHIVE

IFAC PapersOnLine 53-1 (2020) 453–458

Sliding Mode-Based Guidance for UAV Landing on a Stationary or Moving Ground Vehicle

Sashank Modali * **Satadal Ghosh** ** **Sujit P.B.** ***

* *Student, Department of Aerospace Engineering, IIT Madras, Chennai, 600036 India (e-mail: ae16b031@smail.iitm.ac.in.)*
** *Faculty, Department of Aerospace Engineering, IIT Madras, Chennai , 600036 India (e-mail: satadal@iitm.ac.in)*
*** *Faculty, Department of Electronics and Communications Engineering, IIIT Delhi, New Delhi, 110020 India (e-mail: sujit@iiitd.ac.in)*

Abstract: In this paper, the problem of guidance formulation for autonomous landing of unmanned aerial vehicles on stationary or moving or maneuvering ground vehicles at desired approach angles is considered. Nonlinear engagement kinematics have been used. While integrated nonlinear controllers have been developed in the literature for this purpose, the controller inputs often need modification of the existing autopilot structure, which is challenging. In order to avoid that, a higher-level guidance algorithm is designed in this paper leveraging a sliding mode control-based approach. In the presented guidance formulation, target-state-dependent singularity can be avoided in the guidance command. The effectiveness of the presented guidance law is verified with numerical simulation studies.

Keywords: Autonomous Landing, Guidance, Sliding mode control, Non-maneuvering and maneuvering target, Approach angle

1. INTRODUCTION

Unmanned aerial vehicles (UAVs) have become an essential tool for civilian applications (Geng et al. (2013); Waharte and Trigoni (2010)) due to simplicity in their operations and easy availability in the market. Often they are used in critical applications like search and rescue and delivery (medicine, food supplies) operations. Due to limited fuel or battery resources, these vehicles need to land accurately in constrained environments while performing these operations. Although currently the landing is performed manually in most occasions, manual intervention may not be always possible. Also, these vehicles may need to land on moving vehicles which is challenging even for manual operations. Therefore, there is a need to develop autonomous landing solutions for UAVs so that they can land accurately on stationary as well as on moving platforms. Further, it is desirable that the vehicle needs to land in certain approach angles only due to environmental constraints.

There are two components in landing – target (or landing pad) detection and tracking the target (Gautam et al. (2014)). One can use different kinds of sensor information for target detection, for example, camera (Gautam et al. (2017); Saripalli et al. (2002); Cesetti et al. (2010); Rodriguez-Ramos et al. (2017)), lidar (Arora et al. (2013)), and GPS (Zhang and Yuan (2010); Cho et al. (2007); Hsiao et al. (2003); Skulstad et al. (2015)). In this paper, we assume the target to have a high-end GPS or real-time kinematic positioning-augmented GPS (RTK-GPS) that can provide target location information with centimeter level accuracy (Skulstad et al. (2015)). The target broadcasts the location and velocity information to the vehicle. This system is especially suitable for applications like convoy protection (Oliveira et al. (2016); Ding et al. (2010)).

Once the target information has been acquired, the next task is to design a tracking guidance and control mechanism for the aerial vehicle so that it can land on the target. Although, one can design an integrated controller for landing using nonlinear techniques (Voos (2009); Ahmed and Pota (2008); Vlantis et al. (2015); Ghommam and Saad (2017)), the derived control inputs often needs additional modification of the existing autopilot systems, and modifying the autopilot systems is challenging. Therefore, instead of modifying the autopilot system, an on-board computer is planned to be utilized that would determine suitable guidance commands, which will be sent to the autopilot. Since guidance commands are higher level commands, they will only provide reference to the controllers in the autopilot that will try to achieve the desired guidance command.

Depending on different sensing and tracking mechanism, several guidance laws for landing have been proposed in the literature for fixed-wing vehicles (Byoung-Mun et al. (2007); Kim et al. (2013); Yoon et al. (2009); Borowczyk et al. (2017); Barber et al. (2007); Chandra and Ghosh (2019)). The existing works on quad-rotor landing except a few (Ghommam and Saad (2017)) are limited to vertical landing only. Vertical landing techniques may be applica-

10.1016/j.ifacol.2020.06.076

ble for landing on stationary targets, but not for moving targets. Considering that sliding mode control theory has been gainfully leveraged in visual servoing (Lee et al. (2012)) and interceptor-target engagements (Kumar et al. (2012); Rao and Ghose (2013)), in this paper a novel guidance scheme inspired by sliding mode philosophy is adopted for landing a UAV on a moving vehicle. This guidance takes the advantage of sliding mode control theory for planning trajectories, and at the same time can be used in the on-board computer, thus not interfering with the autopilot system. Suitable consideration of multiple sliding surfaces leads to avoiding target-state-dependent singularity in the guidance command.

The rest of the paper is organized as follows. In Section 2, the landing problem formulation is described. In Section 3 the guidance design strategy is described, while a detailed discussion on the synthesized guidance algorithm is presented in Section 4. Effectiveness of the proposed guidance law is demonstrated in Section 5 using simulation studies over different kinds of ground target platforms. Finally, in Section 6 conclusions and possible future works are discussed.

2. PROBLEM FORMULATION

2.1 Goal for Landing Guidance

In this paper the problem of autonomous landing is considered in which a UAV initiates its movement from an arbitrary initial position in three dimensional (3-D) space sufficiently close to a UGV (target) moving in the horizontal (x-y) plane. A guidance algorithm is to be developed for the UAV's motion to achieve the final goal of approaching the UGV and landing on it with zero relative terminal velocity while maintaining a pre-specified terminal line-of-sight (LOS) angle on x-y plane.

An illustrative engagement scenario is shown in Fig. 1. Here, R, R_{xy}, R_z represent the distance between the target and the UAV, its component when projected on the x-y plane and the vertical range between the UAV and the target, respectively. The UAV's speed, flight path angle and heading on x-y plane are denoted as V_p, γ and α_p, respectively. Here, γ is defined such that it lies in the interval, $[-\frac{\pi}{2}, \frac{\pi}{2}]$ rad. In general, [-π, π) rad of angles convention is followed in this paper. The UGV's speed and heading are given as V_t and α_t, respectively. Here, θ denotes the angle between the LOS and the x-y plane. The kinematics is decomposed into in x-y plane and vertical direction (z axis).

The objective of the guidance law is to achieve,

$$\lim_{t\to\infty} R_{xy} = 0;\ \lim_{t\to\infty} R_z = 0;\ \lim_{t\to\infty} \dot{R}_{xy} = 0;\ \lim_{t\to\infty} \dot{R}_z = 0;\ \lim_{t\to\infty} \psi = \alpha_t + \zeta \quad (1)$$

Note that the first four objectives are required for a smooth landing. The final objective dictates a desired approach angle, which is defined here as a desired LOS angle on the x-y plane (ψ). Note that this is different from usual definition of impact angle.

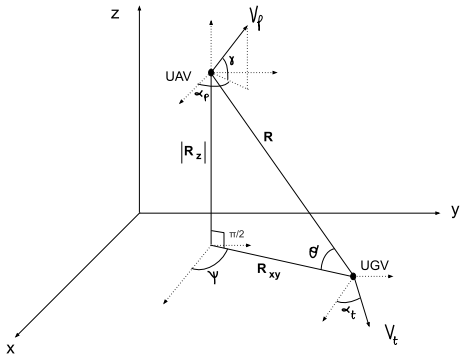

Fig. 1. UAV-target 3D engagement geometry for landing

2.2 Equations of Motion

The 3-D engagement kinematics of the UAV and the ground target (UGV) is represented as below, where $\dot{V}_p$, $\dot{\alpha_p}$ and $\dot{\gamma}$ are the guidance control inputs. Note that the system is control affine.

$$\dot{R}_{xy} = V_t cos(\alpha_t - \psi) - V_p cos(\gamma) cos(\alpha_p - \psi) \quad (2)$$

$$\dot{\psi} = \frac{1}{R_{xy}}(V_t sin(\alpha_t - \psi) - V_p cos(\gamma) sin(\alpha_p - \psi)) \quad (3)$$

$$\dot{R} = \frac{1}{R}(R_{xy}\dot{R}_{xy} + R_z\dot{R}_z) \quad (4)$$

$$\dot{R}_z = -V_p sin(\gamma) \quad (5)$$

$$\dot{\theta} = \frac{1}{R}(V_p\ sin(\gamma)\ cos(\theta) - \dot{R}_{xy}\ sin(\theta)) \quad (6)$$

$$\begin{bmatrix}\dot{V_p} & \dot{\alpha_p} & \dot{\gamma}\end{bmatrix}^T = U \quad (7)$$

Collision course between the UGV and UAV is given as,

$$V_t\ sin(\alpha_t - \psi) = V_p\ cos(\gamma)\ sin(\alpha_p - \psi) \quad (8)$$

From (1), for smooth landing, $\dot{R}_{xy} = 0$ and $\dot{R}_z = 0$ need to be satisfied. From (2), this implies,

$$V_t\ cos(\alpha_t - \psi) = V_p\ cos(\gamma)\ cos(\alpha_p - \psi) \quad (9)$$

And, from (5), the terminal condition $\dot{R}_z = 0$ implies terminal $V_p = 0$ (meaningful for stationary target) or terminal $\gamma = 0$ (meaningful for moving target). Solving Eqs. (5), (8), and (9), the desired terminal velocity and heading of the UAV are obtained. Thus, for terminal $V_t = 0$, we obtain $V_p\ cos(\gamma) = 0$. Else if terminal $V_t \neq 0$,

$$\lim_{R\to 0} V_p = V_t\ \ ,\ \ \lim_{R\to 0} \alpha_p - \alpha_t = 0,\ \ and\ \ \lim_{R\to 0} \gamma = 0 \quad (10)$$

3. GUIDANCE LAW DESIGN

3.1 Synthesis of Guidance Command

The terminal requirements of $\dot{R}_{xy} = 0$, $\dot{R}_z = 0$ and $\psi = \alpha_t + \zeta$ along with zero miss distance (see (1)) form the basic consideration behind the formulation of sliding variables for deriving a suitable guidance law for smooth landing during touchdown on the UGV as shown below.

$$S = \begin{bmatrix} \dot{R}_{xy} + k_a R_{xy} \\ \dot{R}_z + k_a R_z \\ (\dot{\psi} - \dot{\alpha_t}) + k_b(\psi - (\alpha_t + \zeta)) \end{bmatrix} = \begin{bmatrix}(S_1)\\(S_2)\\(S_3)\end{bmatrix} \quad (11)$$

where, k_a and k_b are tuning parameters in the designed guidance law. Now, the guidance is applied such that the sliding variables vary in the following way.

$$\dot{S} = -\begin{bmatrix} k1 & 0 & 0 \\ 0 & k2 & 0 \\ 0 & 0 & k3 \end{bmatrix} \begin{bmatrix} (S_1)^{n/m} \\ (S_2)^{n/m} \\ (S_3)^{n/m} \end{bmatrix} \tag{12}$$

where, k_1, k_2, k_3, m and n are other tuning parameters in the designed guidance law. Among all these tuning parameters, m and n should be odd and co-prime integers such that $0 < n < m$. A discussion on selection of other tuning parameters is provided in section (3.2). Now, from (12), for $i = 1, 2, 3$,

$$(S_i(t))^{\frac{(m-n)}{m}} = (S_i(0))^{\frac{(m-n)}{m}} - \frac{(m-n)}{m}\, K_i\, t \tag{13}$$

Clearly, the dynamics of the sliding variables chosen are finite time convergent. Unlike the signum function of sliding variables, usually considered in sliding mode-based control literature, this form of sliding mode dynamics is helpful to reduce chattering.

From (11) note that R_{xy} and R_z approach zero exponentially as S_1 and S_2 are equal to zero, respectively, and ψ approaches to $\alpha_t + \zeta$ exponentially as S_3 is equal to zero. Thus, the guidance algorithm that ascertains (11) enables a UAV to successfully land on a ground target at a desired approach angle.

3.2 Guidance Command Inputs

Eqs. (2) - (7), (11) and (12), when expanded lead to a system of 3 equations, expressed as $AU = B$. Here U is as given in Eq. (7), and matrices A and B are given by,

$$A = \begin{bmatrix} -cos(\alpha_p - \psi)cos(\gamma) & V_p sin(\alpha_p - \psi)cos(\gamma) & V_p cos(\alpha_p - \psi)sin(\gamma) \\ -sin(\gamma) & 0 & -V_p cos(\gamma) \\ -sin(\alpha_p - \psi)cos(\gamma) & -V_p cos(\alpha_p - \psi)cos(\gamma) & V_p sin(\alpha_p - \psi)sin(\gamma) \end{bmatrix} \tag{14}$$

$$and \;\; B = \begin{bmatrix} -k_1\ (S_1)^{n/m} + V_p\ sin(\alpha_p - \psi)\ cos(\gamma)\dot{\psi} - \\ \dot{V}_t\ cos(\alpha_t - \psi) + V_t\ sin(\alpha_t - \psi)(\dot{\alpha}_t - \dot{\psi}) - \\ ka\ (V_t\ cos(\alpha_t - \psi) - V_p\ cos(\gamma)\ cos(\alpha_p - \psi)) \\ -k_2\ (S_2)^{n/m} + k_a\ V_p\ sin(\gamma) \\ -R_{xy}\ k_3\ (S_3)^{n/m} - k_b\ R_{xy}\ (\dot{\psi} - \dot{\alpha_t}) + \\ \ddot{\alpha_t}\ R_{xy} + \dot{R}_{xy}\dot{\psi} - V_p\ cos(\alpha_p - \psi)\ cos(\gamma)\ \dot{\psi} - \\ V_t\ cos(\alpha_t - \psi)\ (\dot{\alpha}_t - \dot{\psi}) - \dot{V}_t\ sin(\alpha_t - \psi) \end{bmatrix} \tag{15}$$

From (14) and (15), the guidance command inputs are obtained as a solution to the system of equations, $AU = B$. Note that $\det(A) = (V_p)^2 \cos(\gamma)$. When $V_p \neq 0$ and $\cos(\gamma) \neq 0$, the solution to the system is given by,

$$U = A^{-1}B \tag{16}$$

Note that the determinant of matrix A, as shown above, doesn't depend on the target's heading and position directly. Also, $\det(A) = 0$ if and only if $V_p = 0$ or $\cos(\gamma) = 0$. Note that this guidance could avoid target-state-dependent singularity although it might encounter UAV-state-dependent singularity as stated above, which could occur in the following situations :

- Landing on a stationary ground target.
- Vertical takeoff.
- Target moves towards the UAV.

Thus, (16) leads to a non-singular guidance command in almost all scenarios except a few scenarios mentioned above. These situations can generally be handled by suitable manipulation of the inputs. Overall, the guidance algorithm is formulated as,

Algorithm 1 Input Summary

if $\det(A) > \epsilon$ **then**
$U = A^{-1}B$, where $\epsilon < 1$ is a constant
else
  if $V_p < M_1$ **then**
    $\dot{V_p}' = N_1$
  else
    $\dot{V_p}' = 0$
  end if
  if $cos(\gamma) < M_2$ **then**
    $\dot{\gamma}' = -N_2\ sign(\gamma)$
  else
    $\dot{\gamma}' = 0$
  end if
  $U = [\dot{V_p}' \quad 0 \quad \dot{\gamma}']^T$
end if

Values of pre-specified constants ϵ, M_1 and M_2 could be very small, while those of N_1 and N_2 could be big enough to get out of the UAV-state-dependent singularity zone.

4. DISCUSSION ON DESIGNED GUIDANCE LAW

Discussions on the landing guidance algorithm will be presented in this section. They would be based on the premise that the dynamics of the sliding variables are achievable.

From (11) it is evident that if both S_1 and S_2 are zero, then $\dot{R}_z/\dot{R}_{xy} = R_z/R_{xy}$, which implies that θ remains constant. This could be helpful in case of Field-of-View (FOV)-constrained landing.

Next, a discussion on tuning of the guidance parameters, namely, k_1, k_2, k_3, k_a, k_b, m and n, would be presented. Expanding Eq. (16), we obtain :

$$\begin{aligned} \dot{V}_p = {} & k_3 R_{xy}\, cos(\gamma) sin(\alpha_p - \psi)(S_3)^{n/m} + k_2\ (S_2)^{n/m} sin(\gamma) \\ & + k_b\ R_{xy}\ (\dot{\psi} - \dot{\alpha_t})\ cos(\gamma)\ sin(\alpha_p - \psi) - k_a\ V_p\ (sin(\gamma))^2 + \\ & k_a\ \dot{R}_{xy}\, cos(\gamma)\ cos(\alpha_p - \psi) + k_1\ (S_1)^{n/m}\ cos(\gamma)\ cos(\alpha_p - \psi) - \\ & \ddot{\alpha_t}\ R_{xy}\ cos(\gamma)\ sin(\alpha_p - \psi) - \dot{R_{xy}}\ \dot{\psi}\ cos(\gamma)\ sin(\alpha_p - \psi) + \\ & \dot{V}_t\ cos(\gamma)\ cos(\alpha_p - \alpha_t) + V_t\ cos(\gamma)\ (\dot{\alpha_t} - \dot{\psi})\ sin(\alpha_p - \alpha_t) \end{aligned} \tag{17}$$

$$\begin{aligned} \dot{\alpha_p} = \frac{1}{V_p\ cos(\gamma)} [& k_1\ (S_1)^{n/m}\ sin(\alpha_p - \psi) + \\ & k_3\ (S_3)^{n/m}\ R_{xy}\ cos(\alpha_p - \psi) - \\ & \dot{R}_{xy}\ cos(\alpha_p - \psi) - \ddot{\alpha_t}\ R_{xy}\ cos(\alpha_p - \psi) + \\ & k_b\ R_{xy}\ (\dot{\psi} - \dot{\alpha_t})\ cos(\alpha_p - \psi) + \\ & k_a\ V_p\ cos(\gamma)\ cos(\alpha_t - \psi)\ sin(\alpha_p - \psi) - \\ & k_a\ V_t\ cos(\alpha_t - \psi)\ sin(\alpha_p - \psi) + V_p\ cos(\gamma)\ (\dot{\psi}) + \\ & \dot{V}_t\ sin(\alpha_t - \alpha_p) + V_t cos(\alpha_t - \alpha_p)\ (\dot{\alpha_t} - \dot{\psi})] \end{aligned} \tag{18}$$

$$\dot{\gamma} = \frac{-tan(\gamma)}{V_p}\ \dot{V_p} + \frac{k_2\ (S_2)^{n/m} - k_a\ V_p\ sin(\gamma)}{V_p\ cos(\gamma)} \quad (19)$$

As can be seen from Eqs. (17) - (19), the expressions of guidance command inputs $\dot{V_p}$, $\dot{\alpha_p}$ and $\dot{\gamma}$ are not easily tractable. However, considering the dynamics of the sliding variables and associated guidance objectives, the followings are obtained.

First, it is desired that $S_1 \to 0$ before $Rxy \to 0$, to avoid shooting up of $\dot{\psi}$. From Eq. (13) the time for S_1 to reach the sliding surface $S_1 = 0$ can be obtained as,

$$t_{reach_1} = \frac{m}{(m-n)}\ \frac{(S_1(0))^{((m-n)/m)}}{k_1} \quad (20)$$

Differentiating both sides of first row of (11),

$$\ddot{R}_{xy} = -k_a \dot{R}_{xy} - k_1 (S_1)^{n/m} \quad (21)$$

It should be noted that once the system is on the sliding surface, both $|\dot{R}_{xy}(t)|$ and $R_{xy}(t)$ decrease until they become zero. For the subsequent discussion, it is assumed that the guidance is initiated with $\dot{R}_{xy0} < 0$. This can be further divided into 2 sub-cases: $|\dot{R}_{xy0}| > k_a R_{xy0}$ and $|\dot{R}_{xy0}| < k_a R_{xy0}$.

In the first sub-case, $S_{10} < 0$. Then, $S_1(t) < 0$ and $\dot{S}_1(t) > 0$ (from Eq. (12)) throughout the reaching phase, in which the system is reaching the sliding surface. Clearly, from Eq. (21), $\ddot{R}_{xy0} > 0$. This along with $\dot{R}_{xy0} < 0$ and $\dot{S}_1 > 0$ implies that $\dot{R}_{xy}$ remains negative at any time-instant during the reaching phase, which in turn from from eqs. (12) and (21) again imply that $\ddot{R}_{xy}$ remains positive at any time-instant during this phase. Thus,

$$|\dot{R}_{xy}| \leq |\dot{R}_{xy0}| \leq max(|\dot{R}_{xy0}|, k_a R_{xy0}) \quad (22)$$

In the second sub-case, $S_{10} > 0$. Therefore, following (12), $\dot{S_1}(t) < 0$ and $S_1(t) > 0$ throughout the reaching phase. At any time-instant t during the reaching phase, if $\dot{R}_{xy}(t) = 0$, from Eq. (21), this implies that $\ddot{R}_{xy}(t) \leq 0$. This leads to a contradiction for $\dot{R}_{xy0} < 0$. Therefore, once $\dot{R}_{xy0} < 0$ is satisfied, $\dot{R}_{xy}$ is always negative and doesn't reach zero throughout this phase. This implies $k_a R_{xy}(t) < k_a R_{xy0}$. Since $S_1(t) > 0$, $|R_{xy}(t)| < k_a R_{xy}(t) < k_a R_{xy0}$. Thus,

$$|\dot{R}_{xy}| \leq |k_a R_{xy0}| \leq max(|\dot{R}_{xy0}|, k_a R_{xy0}) \quad (23)$$

The above arguments give a lower bound on the time taken for the range between the UAV and the ground target in the x-y plane to reach zero. This is given by,

$$t_{R_1} \geq \frac{R_{xy0}}{max(\ |\dot{R}_{xy0}|\ ,\ K_a\ R_{xy0})} \quad (24)$$

With the consideration of desired t_{reach_1} to be less than t_{R_1}, a sufficient condition is derived as below from (20) and (24).

$$k_1 \geq \frac{m}{(m-n)} \frac{(S_{10})^{((m-n)/m)}}{R_{xy0}} \max(|\dot{R}_{xy0}|, k_a R_{xy0}) \quad (25)$$

Next, consider selection criteria of k_2 and k_3. Note that in regular landing problem initial value of R_z is quite high. Also, from the dynamics in Eq. (3), $\dot{\psi}$ shoots up as $Rxy \to 0$. Therefore, to avoid this, the selection of k_1 is done and is considered as a benchmark for selecting k_2 and k_3 such that all sliding variables become zero in same time. This simplifies the selection criteria as follows.

$$\frac{k_2}{k_1} = (\frac{S_{20}}{S_{10}})^{((m-n)/m)}\ ,\ \frac{k_3}{k_1} = (\frac{S_{30}}{S_{10}})^{((m-n)/m)} \quad (26)$$

Next, consider selection criteria of m and n. Recall that m and n were considered as odd and co-prime positive integers ($0 < n < m$) in Section 3.1. Besides this, it may be noted that because of the enforced dynamics of sliding variables in (12), the guidance input $\dot{\alpha_p}$ in (16) could shoot up due to the presence of terms such as $(S_3)^{n/m} R_{xy}$, as the sliding variables approach sufficiently close to zero if $n/m << 1$. In order to avoid that n/m should be chosen quite close to 1.

Finally, consider the selection criteria of k_a and k_b. Since the desired LOS angle in the x-y plane is to be achieved at the time of landing, it is desired that ψ approaches $\alpha_t + \zeta$ faster on the sliding surface $S_3 = 0$ than R_{xy} and R_z approaches to zero on the sliding surfaces $S_1 = 0$ and $S_2 = 0$, respectively. This leads to the following selection criterion.

$$k_b \geq k_a \quad (27)$$

However, k_a and k_b are to be chosen judiciously such that the guidance command inputs are within acceptable limits.

5. SIMULATION RESULTS

MATLAB simulations are presented in this section assuming point mass models of the UAV and the UGV. As per the developed guidance algorithm, the UAV generates three commanded inputs to the UAV control block. Though the guidance is formulated for all-aspect planar targets, simulations are presented for two cases of interest, namely, stationary and circular trajectories of the ground target. In both the cases considered, the initial speed of the UAV is taken as 5 m/s. The UAV starts, at a distance of 15 m from the target, with $R_{xy0} = 7.5$ m and $R_{z0} = 7.5\sqrt{3}$ m. The initial heading and flight path angles of the UAV are taken as $-\pi/6$ and 0 rad respectively. The initial LOS angle projected to the (xy)-plane (ψ_0) is taken as $-\pi/6$ rad. In the cases of moving target, the target speed is fixed at 3 m/s for the purpose of simulation. Also, for the purpose of simulation, the parameters m and n are chosen as $m = 5$, $n = 3$; and the constants, k_b and k_a, are chosen such that $k_b = 2k_a = 0.4$.

The results of the simulations are given in figures (2) to (6). From the simulations, it can be noted that for moving targets (terminal $V_t \neq 0$), the desired speed, LOS angle on x-y plane and the heading angle on x-y plane, given in Eq. (10), are achieved in steady state as shown in Fig. 5.

5.1 Stationary Targets

It has been mentioned that, unique solutions to the system of equations, are feasible when $V_p \neq 0$ and $cos(\gamma) \neq 0$. In the case of stationary targets, during collision course, $V_p \to 0$ as $R \to 0$, for a smooth landing. This poses a problem in the end game phase, where the control vector may blow up. But, as shown in Alg. (1) , it is still possible to reach the target with a small error in position. This

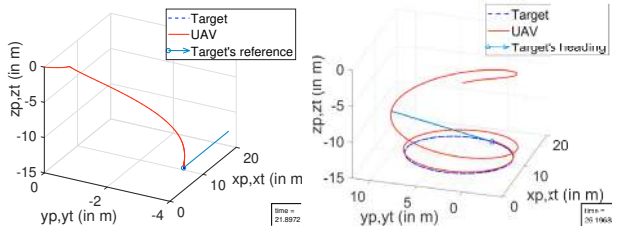

(a) Stationary Target (b) Constant Maneuvering Target

Fig. 2. Trajectory plots for UAV and target

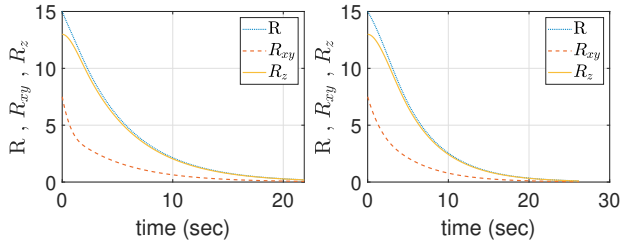

(a) Stationary Target (b) Constant Maneuvering Target

Fig. 3. LOS distance in 3-D and x-y,z projections

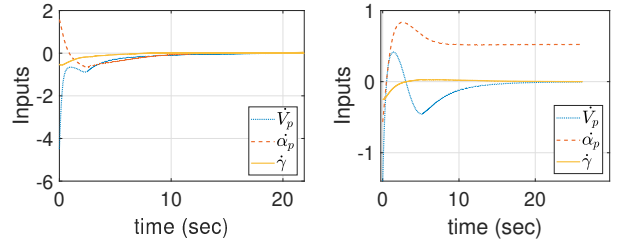

(a) Stationary Target (b) Constant Maneuvering Target

Fig. 4. Inputs for UAV

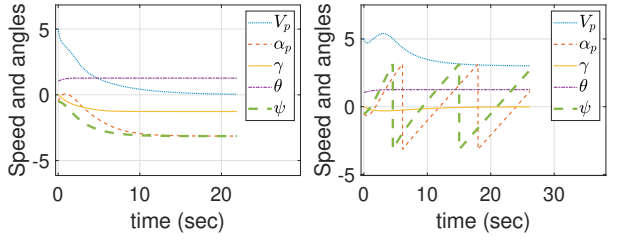

(a) Stationary Target (b) Constant Maneuvering Target

Fig. 5. UAV Speed and angles

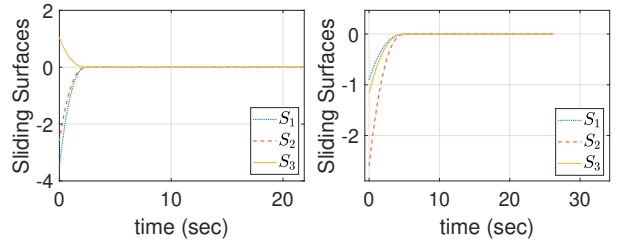

(a) Stationary Target (b) Constant Maneuvering Target

Fig. 6. Sliding surfaces with time

is shown in the simulations. The desired approach angle is given as π. The tuning parameters as obtained from section 4 are given by, $k_1 = 1.6505$, $k_2 = 1.4651$, $k_3 = 1.0186$

The UAV reaches the target at a position error of 0.2 m only. The maximum speed is observed to be 5 m/s and the maximum rate of change in the speed is observed to be -4.5 m/s^2. The maximum rate of change in the heading of the UAV is observed to be $\pi/2$ rad/s. The approach angle at impact is 0.998 π rad, which is very close to the desired approach angle. The time taken for landing is 21.91 sec.

5.2 Constant Maneuvering Target

In this example, the target executes a circular motion with $\dot{\alpha_t} = \pi/6$ rad/sec. All other initial conditions are kept same as before. The desired approach angle in the (xy)-plane is considered as $\pi/2$ rad. The tuning parameters as obtained from section 4 are given by, $k_1 = 0.46095$, $k_2 = 0.7038$, $k_3 = 0.51001$

In the simulation, the maximum speed observed for the UAV is 5.3971 m/s. The maximum rate of change of the UAV's heading is observed to be 0.8344 rad/s and that of its speed is observed to be -1.40 m/s^2. The approach angle at impact is 0.499995 π rad. The time taken for landing is 26.20 sec.

6. CONCLUSION

A novel approach angle-constrained guidance law inspired by the sliding mode control philosophy has been presented in this paper for autonomous landing of a UAV on stationary or moving or maneuvering ground targets to show that the sliding mode control philosophy is a useful tool for planning trajectories and dealing with constraints in real-world scenarios. Stability analysis and a detailed discussion on the selection of guidance parameters have also been presented. By numerical simulation studies the guidance law has been shown to effectively achieve soft landing on stationary and maneuvering targets at desired approach angles. Future works involve experimental validation of the presented guidance algorithm on real test-beds and improvements in the guidance formulation.

REFERENCES

Ahmed, B. and Pota, H.R. (2008). Backstepping-based landing control of a ruav using tether incorporating flapping correction dynamics. In *American Control Conference*, 2728–2733. Seattle, Washington, USA.

Arora, S., Jain, S., Scherer, S., Nuske, S., Chamberlain, L., and Singh, S. (2013). Infrastructure-free shipdeck tracking for autonomous landing. In *IEEE International Conference on Robotics and Automation*, 323–330. Karlsruhe, Germany.

Barber, D.B., Griffiths, S.R., McLain, T.W., and Beard, R.W. (2007). Autonomous landing of miniature aerial vehicles. *Journal of Aerospace Computing, Information, and Communication*, 4(5), 770–784.

Borowczyk, A., Nguyen, D.T., Nguyen, A.P.V., Nguyen, D.Q., Saussié, D., and Le Ny, J. (2017). Autonomous landing of a quadcopter on a high-speed ground vehicle. *Journal of Guidance, Control, and Dynamics*, 40(9), 2378–2385.

Byoung-Mun, M., Min-Jea, T., David Hyunchul, S., and HyoChoong, B. (2007). Guidance law for vision-based automatic landing of uav. *International Journal of Aeronautical and Space Sciences*, 8(1), 46–53.

Cesetti, A., Frontoni, E., Mancini, A., Zingaretti, P., and Longhi, S. (2010). *A Vision-Based Guidance System for UAV Navigation and Safe Landing using Natural Landmarks*, 233–257. Springer Netherlands, Dordrecht.

Chandra, K.R. and Ghosh, S. (2019). Hu-moment-based autonomous landing of a uav on a hemispherical dome. In *2019 International Conference on Unmanned Aircraft Systems (ICUAS)*, 19–25. IEEE.

Cho, A., Kim, J., Lee, S., Choi, S., Lee, B., Kim, B., Park, N., Kim, D., and Kee, C. (2007). Fully automatic taxiing, takeoff and landing of a uav using a single-antenna gps receiver only. In *International Conference on Control, Automation and Systems*, 821–825.

Ding, X.C., Rahmani, A.R., and Egerstedt, M. (2010). Multi-uav convoy protection: An optimal approach to path planning and coordination. *IEEE Transactions on Robotics*, 26(2), 256–268.

Gautam, A., Sujit, P., and Saripalli, S. (2014). A survey of autonomous landing techniques for uavs. In *International Conference on Unmanned Aircraft Systems*, 1210–1218. Orlando, USA. doi:10.1109/ICUAS.2014.6842377.

Gautam, A., Sujit, P., and Saripalli, S. (2017). Autonomous quadrotor landing using vision and pursuit guidance. *IFAC-PapersOnLine*, 50(1), 10501–10506.

Geng, L., Zhang, Y.F., Wang, J.J., Fuh, J.Y.H., and Teo, S.H. (2013). Mission planning of autonomous uavs for urban surveillance with evolutionary algorithms. In *IEEE International Conference on Control and Automation*, 828–833. Hang Zhou, China.

Ghommam, J. and Saad, M. (2017). Autonomous landing of a quadrotor on a moving platform. *IEEE Transactions on Aerospace and Electronic Systems*, 53(3), 1504–1519.

Hsiao, F.B., Huang, S.H., and Lee, M.T. (2003). The study of real-timed gps navigation accuracy during approach and landing of an ultralight vehicle. In *International Conference on Recent Advances in Space Technologies*, 375–384.

Kim, H.J., Kim, M., Lim, H., Park, C., Yoon, S., Lee, D., Choi, H., Oh, G., Park, J., and Kim, Y. (2013). Fully autonomous vision-based net-recovery landing system for a fixed-wing uav. *IEEE/ASME Transactions on Mechatronics*, 18(4), 1320–1333.

Kumar, S.R., Rao, S., and Ghose, D. (2012). Sliding-mode guidance and control for all-aspect interceptors with terminal angle constraints. *Journal of Guidance, Control, and Dynamics*, 35(4), 1230–1246.

Lee, D., Ryan, T., and Kim, H.J. (2012). Autonomous landing of a vtol uav on a moving platform using image-based visual servoing. In *2012 IEEE International Conference on Robotics and Automation*, 971–976. doi: 10.1109/ICRA.2012.6224828.

Oliveira, T., Aguiar, A.P., and Encarnacao, P. (2016). Moving path following for unmanned aerial vehicles with applications to single and multiple target tracking problems. *IEEE Transactions on Robotics*, 32(5), 1062–1078.

Rao, S. and Ghose, D. (2013). Sliding mode control-based autopilots for leaderless consensus of unmanned aerial vehicles. *IEEE transactions on control systems technology*, 22(5), 1964–1972.

Rodriguez-Ramos, A., Sampedro, C., Bavle, H., Milosevic, Z., Garcia-Vaquero, A., and Campoy, P. (2017). Towards fully autonomous landing on moving platforms for rotary unmanned aerial vehicles. In *2017 International Conference on Unmanned Aircraft Systems (ICUAS)*, 170–178. IEEE.

Saripalli, S., Montgomery, J.F., and Sukhatme, G.S. (2002). Vision-based autonomous landing of an unmanned aerial vehicle. In *IEEE International Conference on Robotics and Automation*, volume 3, 2799–2804.

Skulstad, R., Syversen, C., Merz, M., Sokolova, N., Fossen, T., and Johansen, T. (2015). Autonomous net recovery of fixed-wing uav with single-frequency carrier-phase differential gnss. *IEEE Aerospace and Electronic Systems Magazine*, 30(5), 18–27.

Vlantis, P., Marantos, P., Bechlioulis, C.P., and Kyriakopoulos, K.J. (2015). Quadrotor landing on an inclined platform of a moving ground vehicle. In *IEEE International Conference on Robotics and Automation (ICRA)*, 2202–2207. Washington, USA.

Voos, H. (2009). Nonlinear control of a quadrotor micro-uav using feedback-linearization. In *IEEE International Conference on Mechatronics*, 1–6. Mulaga, Spain.

Waharte, S. and Trigoni, N. (2010). Supporting search and rescue operations with uavs. In *International Conference on Emerging Security Technologies*, 142–147. Islamabad, Pakistan.

Yoon, S., Jin Kim, H., and Kim, Y. (2009). Spiral landing trajectory and pursuit guidance law design for vision-based net-recovery uav. In *AIAA Guidance, Navigation, and Control Conference and Exhibit*. Chicago, Illinois. doi:10.2514/6.2009-5682.

Zhang, J. and Yuan, H. (2010). Analysis of unmanned aerial vehicle navigation and height control system based on gps. *Journal of Systems Engineering and Electronics*, 21(4), 643–649.